Behavior of Double-Web Angles Beam to column connections

IOP Conf. Series: Materials Science and Engineering **342** (2018) 012023 doi:10.1088/1757-899X/342/1/012023

Behavior of Double-Web Angles Beam to column connections

K Al Fakih, S C Chin and S I Doh

Faculty of Civil Engineering & Earth Resources, Universiti Malaysia Pahang, 26300 Gambang, Pahang, Malaysia.

E-mail: PAC16001@stdmail.ump.edu.my

Abstract. This paper contains the study performed on the behavior of double-web angles by using finite element analysis computer package known as "Abaqus". The aim of this present study was simulating the behavior of double-web angles (DWA) steel connections. The purpose of this article is to provide the basis for the fastest and most economical design and analysis and to ensure the required steel connection strength. This study, started used review method of behavior of steel beam-to-column bolted connections. Two models of different cross-section were examined under the effect of concentrated load and different boundary conditions. In all the studied case, material nonlinearity was accounted. A sample study on DWA connections was carried out using both material and geometric nonlinearities. This object will be of great value to anyone who wants to better understand the behavior of the steel beam to column connection. The results of the study have a field of reference for future research for members of the development of the steel connection approach with simulation model design.

1. Introduction

Many fabricators, manufacturers, and erectors prefer to make a simple connection that can be easily assembled and installed, like bolted joints instead of welded joints. Welding requires more time, combined with a highly skilled workforce. Therefore, many steel manufacturers prefer bolted joints in this area. Steel joints are classified into two types: the first type is partially restrained (PR) and the second type is completely restrained (FR). In the construction of steel joints, it is assumed that the FR joints have sufficient rigidity to maintain the angles between the members of the connection. It is also assumed that the PR connections do not have sufficient stiffness to maintain the angles between the members of the connection (AISC 2011). These connections are leads to the overload resulting from other factors such as welds, loads and gravity. The available experimental results are used to find useful limit states and to improve a rational design procedure for bolted links similar to the links that are considered in this study. The proposed study focuses on the understanding of the behavior of steel joints exposed to shear or moment loads using the finite element method (FEM). The objective of this study is to theoretically provide the moment-rotation characteristics and the corresponding parameters of the semirigid connections between beam and column using the ABAQUS computer software. It affects the flexibility of the connections both of the distribution of forces and of the deformation in columns and beams of the frame. The frame must be calculated in the analysis. It is believed that the flexible analysis of linear distortions is relatively small and that equilibrium equations can be formulated with respect to the initial technique. Several types of research have been conducted on the behavior and design of steel joints. The objective was to provide better understanding and better techniques for evaluating between beams and column joints under the influence of shear and moment loads.

Figure 1 shows the two kinds of connection; the first type is partially restrained (PR) such as top-set angle connection and the second type is completely restrained (FR) such as extended end plate steel connection and the top-set angle with double web angle connection. In addition, can be seen that EP connection and TSA - DWA connections are amongst the stiffest connection [10].

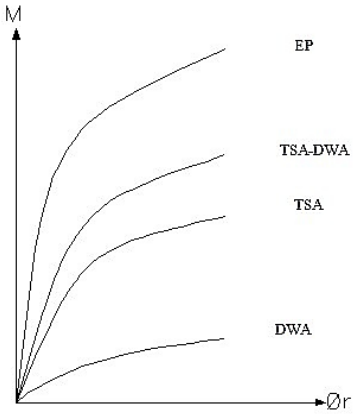

Figure 1. Typical moment rotation curve of beam-to-column connection**s** [10].

Prabha et al. focused on the influence of many factors in the beam/column connection especially in the double web angle connection (DWA), such as air gap effect, angular length, angular thickness and gauge length on the behavior of the links. Three-dimensional (3D) connection moments, plastic-elastic nonlinear finite element analysis, to evaluate the behavior of the DWA connection. Analysis by changing the number of elements in a set of trace models. The proposed equation is compared with the experimental results and the free Morris model was found in full agreement [1]. The design process and the results obtained were presented with the numerical simulation of the upper seat angle with double angle web angles [2]. This was followed by finite element modeling using the ABAQUS program, which is based on previous experimental results. The reference researcher prepared the numerical models of four different configurations according to the program. numerical results from available experimental tests. The distortions and behavior of the virtual sample are the nearly same as those of the existing tests. Ahmed and Hasan proposed a research study for nonlinear finite element analysis (FE) of known set-top angle connections [3]. Performing the simulation 16 samples tests from available references. Compared to the results of the analysis of finite elements with the available experimental results to examine the applicability of the model, the results were close to each other. Sulong et al., nonlinear models were developed for various types of connections using component methods to simulate temperature changes and steel connections at different light load conditions. The model can represent the combination of the typical connection types, the top-set angle with double web angle connection, the double web angle connection, top-seat, extended end plate steel connection. Verification of the proposed connection model is carried out by comparing the analytical simulations with the current results of common tests and by testing joints and lower seats insulated at high-temperature conditions. The results demonstrate the efficiency of identifying the convergence of the proposed model with the power of the communication features and the results of the laboratory test [4]. Abolmaali et al., presented two types of double web angle semi-rigid connections to know the cyclic behavior of such connections: welded with bolted connections and bolted-bolted connections and prestressed bolts for load testing. Cyclic loading was applied to twenty test samples prepared for each test sample using the load control in the initial cycle. Fault modes and moment-rotation hysteresis circuits are provided for all test cases. The results of the experimental tests are verified for all test samples and the cyclic behavior of each test sample is discussed. Two failure modes were observed for the DWA semi-rigid bolted-bolted connections: excessive rotation due to bearing damage and angled bending of the beam bar. Furthermore, this study presented the final moment values, initial rigidity, failure modes and final rotation capacity of the links [5]. Xinwu, examined the behavior of semi-rigid connections under cyclic

inversion load [6]. Liew, et al., studied in part1 and 2, the connection parameters were developed and generalized in the context of angular links, TSA links, DWA with TSA links [7,8]. Hong et al., examined the effect of the angular thickness and the gauge space of bolt, and find the stress distribution and moment-rotation of double-web angle connections of each sample. Samples exposed to shear loads are considered to have a structural strain formed of a perfectly elastic-plastic, that was assumed. ABAQUS software is used to analyze the nonlinear behavior of double-web angled links. Experimental tests were performed with the same material and geometric conditions to verify the analysis of the finite element model. According to the test results, the element models were verified by comparing the moment-rotation curves with the deformed shapes derived from the analysis of model and the available results from literature [9]. The behavior of a connection is explained by the moment-rotation curve. Moment-rotation curves for some connections usually use PRC as shown in Figure 1.
There are many researchers who have studied the behavior of the column connection to beam and simulate it using computer software [11-19].

2. Modeling and Simulation

2.1. Experimental Specimen Description

Based on that experimental data obtained from studies reported by Lewitt et al, which studied the DWA connections [11]. In order to know the behavior of the DWA connection and to test the predictions of the connection model, it was studied and compared with the with the available full-scale test results of connections that have material and component compatibility. Connection components A36 are made of steel and 19.1 mm are made of A325 screws. The connection details of the DWA are shown in Figure 2. In this analysis, the flexible frame study carried out by Lewitt et al., Al, was considered [11]. A summary of the DWA connection geometries is as shown in Tables 1 to 3.

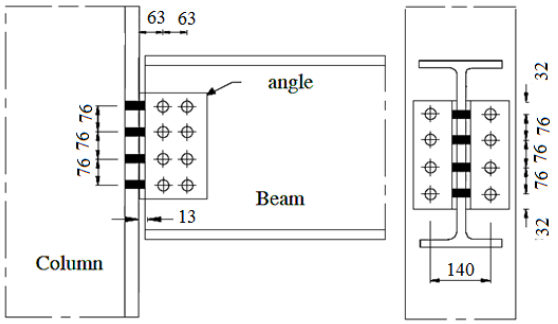

Figure 2. Typical TSA connections [11].

Table 1. Connection geometry of DWE [11]

Test Ref	Beam size mm*kg/m	Column size mm*kg/m	Gage mm	Web-Angle size mm	Fastener mm
FK-3	W310x40	W250x73	66.67	152.4x102x9.5x216	A325-19.1
FK-5	W530x92	W130x97	63.5	152.4x102x11.11x368	A325-19.1

Table 2. Columns geometric dimensions and yield stresses [11]

Test Ref	d mm	b_f mm	t_w mm	t_f mm	A mm	L mm	F_y MPa
FK-3	254	254	8.6	14	5740	1000	248
FK-5	307.8	304.8	9.9	15.4	12320	1000	248

Table 3. Beams geometric dimensions and yield stresses [11]

Test Ref	d mm	b_f mm	t_w mm	t_f mm	A mm	L mm	F_y MPa
FK-3	310	165	5.84	9.65	4995	1200	248
FK-5	533	209	10.2	15.6	9480	1200	248

2.2. Finite Element Modeling

The ABAQUS program can organize and analyze complex problems of connections, including structural problems and three-dimensional structures. In such software, technology lies in finding the right form: the development of the mesh - arrangement. It should balance the size of the mesh - an arrangement between the need for a fine mesh to give an accurate distribution of stress and time reasonable analysis. The perfect solution is to use a fine mesh in high-pressure areas and a coarser mesh in the remaining areas. In all types of connection, the connection is symmetrically arranged about the vertical medial line as shown in Figure 3.

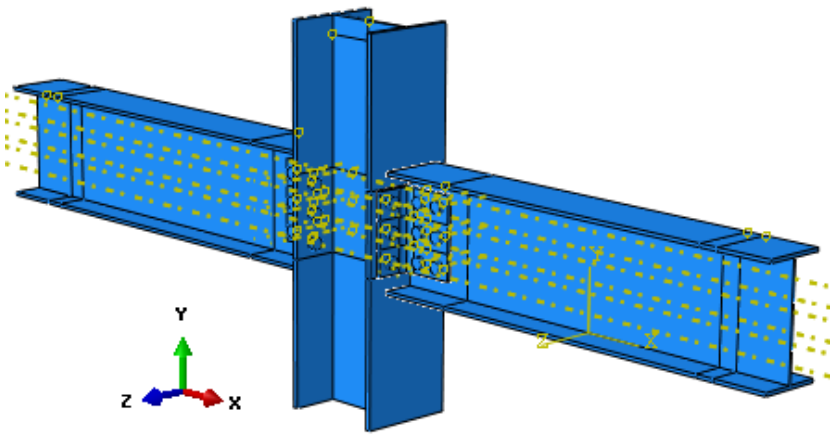

Figure 3. DWA Connections.

2.2.1. Types of elements. In the finite element model, the three-dimensional solid brick element (3D) in ABAQUS was used as shown in Figure 4; consists of eight nodes and each node has three degrees of freedom. This element has the ability to model plasticity, has a large deformation and stress-strain behavior and uses a lower integration method. Bolts, beams, columns and corner elements are modeled using C3D8 elements for the parts. The C3D8 elements are three-dimensional solid hexahedral elements with eight nodes with three degrees of freedom x, y, and z, or 1,2 and 3 respectively, as shown in Figure 4. Referring Figure 5 shows the solid elements C3D8 of the 3D iso-Parametric. 3D iso-parametric solid continuum elements with higher order models are capable of modeling curved boundaries. The elements were numerically integrated, although the C3D8 elements were linear with respect to geometry.

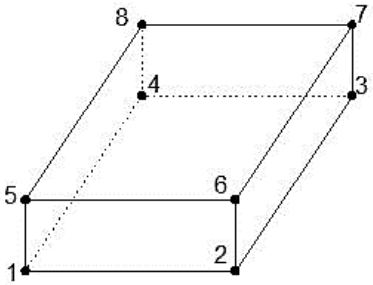

Figure 4. Bolt Solid elements.

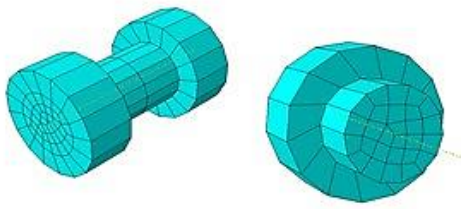

Figure 5. Bolt mesh arrangement.

The complete beam model with final arrangement of mesh discretization is shown in Figure 6.

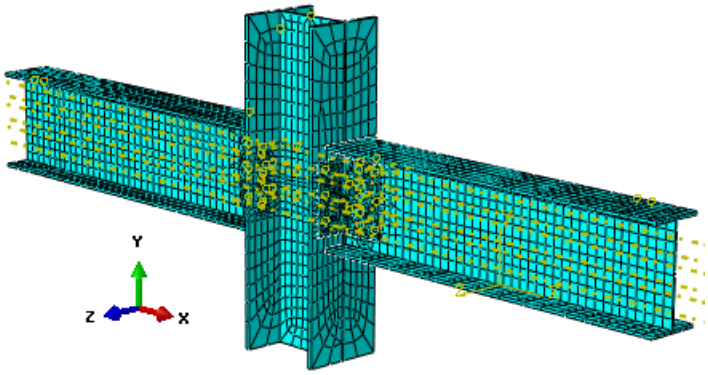

Figure 6. Complete beam models with final arrangement.

2.2.2. *Nonlinear Materials Behaviour.* Nonlinear material definitions play an important role in finite element analysis because each definition of the different parts of the connection must be considered carefully. This means that you need to simulate all the parameters using the basic elements of connection, physical models, and material parameters such as on the beams, columns, and web-angles, flanges, bolts, and nuts. Non-linear material occurs when the stress-strain relationship is not linear so that the steel yield becomes plastic. In fact, carbon steel ASTM A36 mild steel used in the analysis of Azizinamini, et al., may be of different strain-stress diagrams by applying different loading rates and temperature [19]. Otherwise, the loading rate is a specific property. Through the experimental research that has been investigated for analysis in this property where the rate of a load on the connection that has been investigated in the case of a load of monotonous. It was found that the steel takes the lowest yield point and follows almost the exact path of the stress-strain chart as those found in any steel design manual. The figure that explains areas such as stress-strain diagram is shown in Figure 7 for convenience. This graph explains the three phases of the mild carbon steel behaviour from the initial loading whit failure.

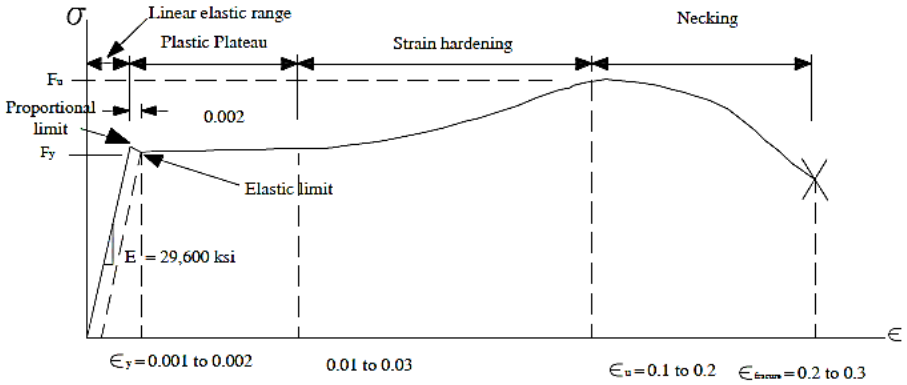

Figure 7. A typical Stress – Strain Diagram for Mild-Carbon Steel [19].

All elements were identified as elastic isotropic properties. The data of test materials were obtained from available all steel tests and the curves allowed stress-strain based on actual values instead of theoretical values. For plastic, elastic data bolts and other elements are defined as shown in Table 4. Von Misses yield performance criteria are used for all kinds of steel connection.

Table 4. Material non-linearity properties.

Tyap of element	Yield stress MPa	Ultimate stress MPa	Modulus of Elasticity Gap	Poisson ritio
Beam, Column and plate	248	483	207	0.3
Bolts	634	828	210	0.3

2.2.3. Boundary Condition. The boundary conditions applied to such connections prevent displacement in X, Y, Z directions. Fig. 8 shows the support boundaries at the end of the package (curve U1 = U2 = U3 = 0).

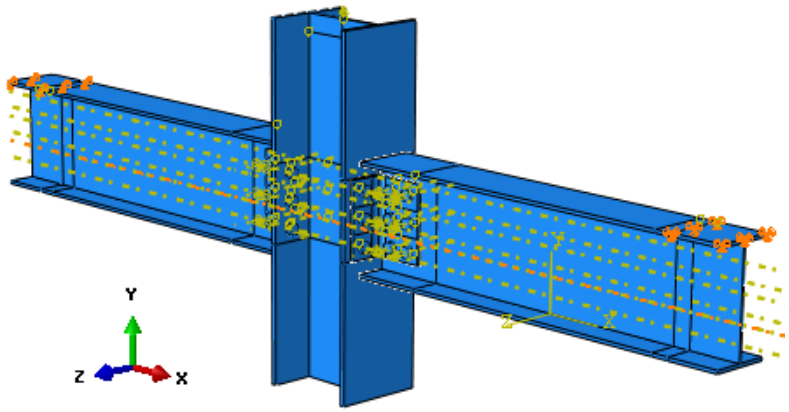

Figure 8. Boundary conditions and loads

2.2.4. Loads. The load was loaded via a concentrated load, at a point in the center of the model. The load is added to the load control file, in the add loading window to achieve the desired size of the bending moments of the connections. The step of the load factor was set to 1 and the maximum load factor was set at 100 at each iteration with the maximum variation of the load factor change automatically. The load applied to sample FK-3 was 36 KN and 144 KN for the sample FK-5 [11].

3. Results

In all cases, the inputs and outputs are based on the description in this section for load factor 1 to 100 set. The maximum load factor of change in each iteration automatically.

3.1. Specimen FK-3.

Using the 1.0 scale factor to make the displacement visible, the deformities shape von-misses stress are plot as shown in Figure 9 and Figure 10.

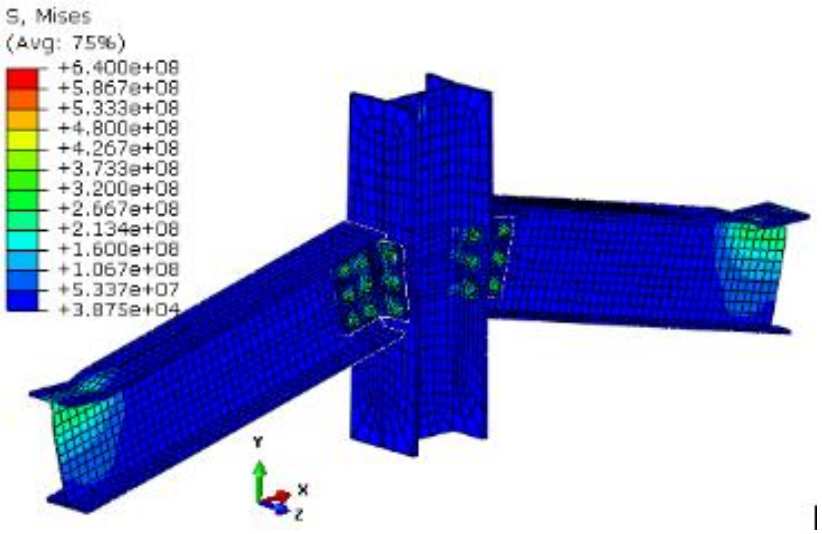

Figure 9. Deformation and Von-Misses stress plot of specimen FK-3.

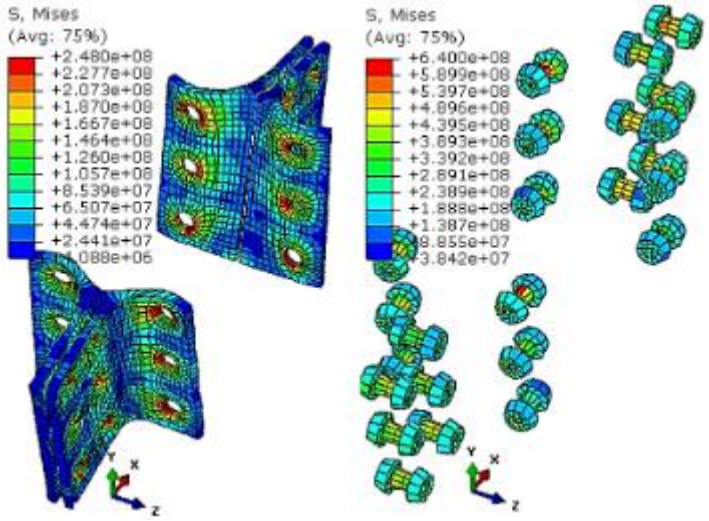

Figure 10. Connection deformation and Von-Misses stress plot of specimen FK-3.

The thick shell element stresses and solid element cannot be in in a single frame because they have different degrees of freedom. Node 6 from the beam was selected for finding the displacement analysis at this node. In addition, the node 6 selected was located at the top of the beam end at 1.2 m from the end support as shown in Figure 11.

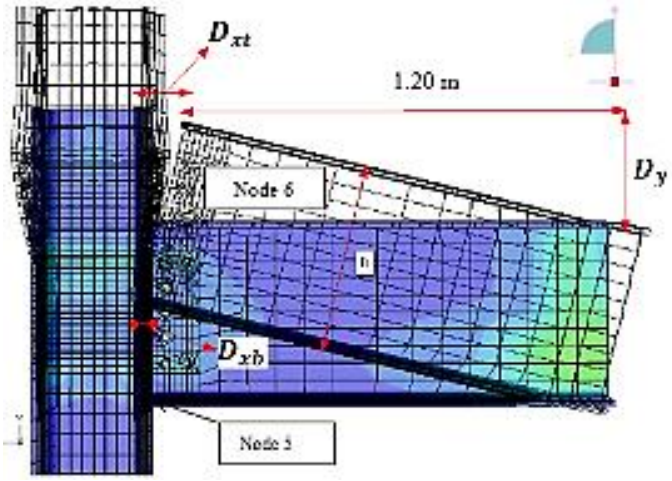

Figure 11. Connection deformed shape showing node 6 and node 5 of specimen DWE.

The connection rotates at Ø as shown in Figure 11.
The connection rotation is defined as

$$\text{Ø} = \tan^{-1}\left[\frac{\Delta x}{h}\right] \quad (1)$$

$$\Delta x = [D_{xt} - D_{xb}] \quad (2)$$

Where:
Ø = the relative rotation of connection.
D_{xt}= the top horizontal displacement of node 6.
D_{xb}= the bottom horizontal displacement of node 5.
h = the beam depth (0.310 m).
The rotation Ø in radian unit, while linear measurements are in meters' unit.
The applied moment was calculated using the following equation:
M = Load factor x 0.5 * L
Where (M) is applied moment in kN.m acting 1.2 m from the support, (L) is the length of the beam.
Numerical results for the calculated loads and displacements are shown in Table 5.

Table 5. Load versus and displacement (D_y) for specimen FK-3.

Load-Step	Displacement -$\boldsymbol{D_y}$ $(\boldsymbol{m})$	Load (kN)
1	0.0000000	0.000
2	0.0000180	0.141
3	0.0000370	0.281
4	0.0000655	0.492
5	0.0001083	0.809
6	0.0001718	1.283
7	0.0002670	1.995
8	0.0004100	3.063
9	0.0006251	4.666
10	0.0009479	7.067
11	0.0014313	10.670
12	0.0021568	16.078
13	0.0060526	24.188
14	0.0098908	27.140
15	0.0155946	30.092
16	0.0226904	33.048
17	0.0307499	36.000

The total vertical displacement against the total load factor graph for node 6 as shown in Figure 12.

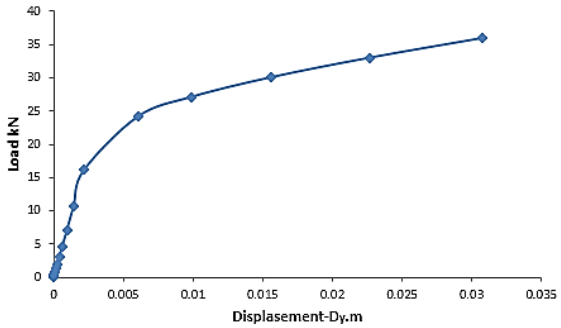

Figure 12. Load -versus vertical displacement D_y at node 6 of specimen FK-3.

Full computer results and the calculated Moment and rotations Ø are shown in Table 6.

Table 6 Calculated moments and corresponding rotations for specimen FK-3.

Load-Step	$\boldsymbol{D_{xt}}$ $(\boldsymbol{m})$	$\boldsymbol{D_{xb}}$ $(\boldsymbol{m})$	$[\Delta_x/\boldsymbol{h}]$	M (kN.m)	Ø (rad)
1	0.0000000	0.0000000	0.0000000	0.000	0.0000000
2	0.0000004	-0.0000048	0.0000167	0.074	0.0000167
3	0.0000009	-0.0000098	0.0000343	0.148	0.0000343
4	0.0000015	-0.0000173	0.0000607	0.258	0.0000606
5	0.0000025	-0.0000286	0.0001003	0.425	0.0001003
6	0.0000040	-0.0000453	0.0001591	0.674	0.0001591
7	0.0000062	-0.0000705	0.0002474	1.047	0.0002473
8	0.0000096	-0.0001082	0.0003798	1.608	0.0003796
9	0.0000146	-0.0001650	0.0005791	2.449	0.0005788
10	0.0000220	-0.0002501	0.0008779	3.710	0.0008775
11	0.0000333	-0.0003776	0.0013252	5.602	0.0013246
12	0.0000501	-0.0005688	0.0019964	8.441	0.0019954
13	0.0000826	-0.0016284	0.0055196	12.699	0.0055168
14	0.0001000	-0.0026792	0.0089651	14.249	0.0089605
15	0.0001235	-0.0042432	0.0140861	15.799	0.0140790
16	0.0001518	-0.0061905	0.0204590	17.350	0.0204486
17	0.0001838	-0.0084037	0.0277016	18.900	0.0276875

The moment-rotation (M-Ø) curve for specimen FK-3 is shown in Figure 13. These diagrams are used to calculate the rotation of the beam and the column.

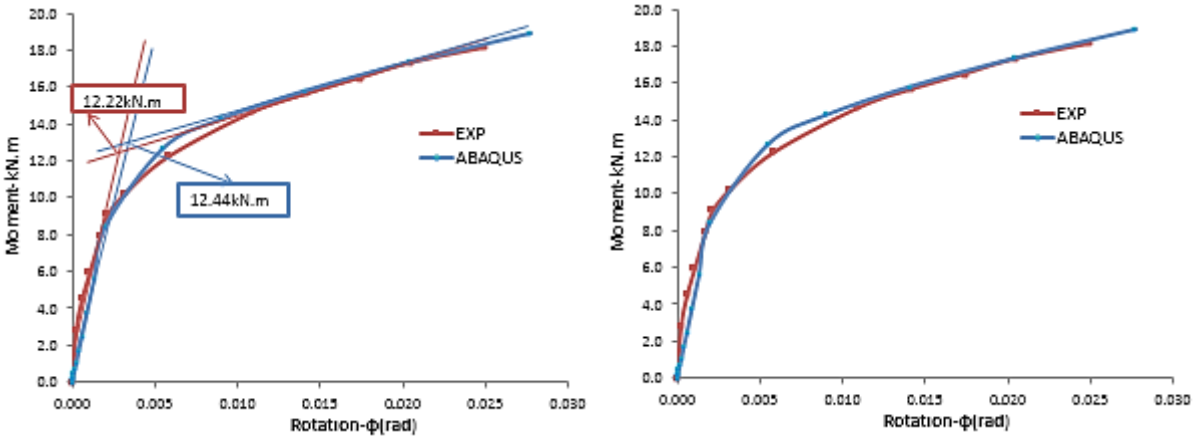

Figure 13. Moment-Rotation (M-Ø) curve for specimen FK-3.

3.2. Specimen FK-5.

Using the 1.0 scale factor to make the displacement visible, the deformities shape von-misses stress are plot as shown in Figure 14 and Figure 15.

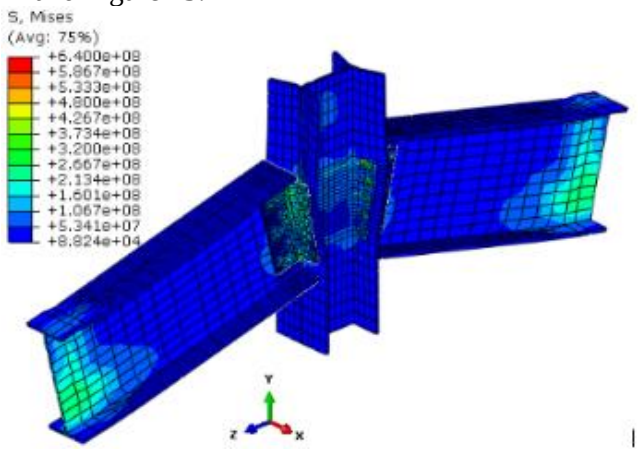

Figure 14. Deformation and Von-Misses Stress of connection plot of specimen FK-5.

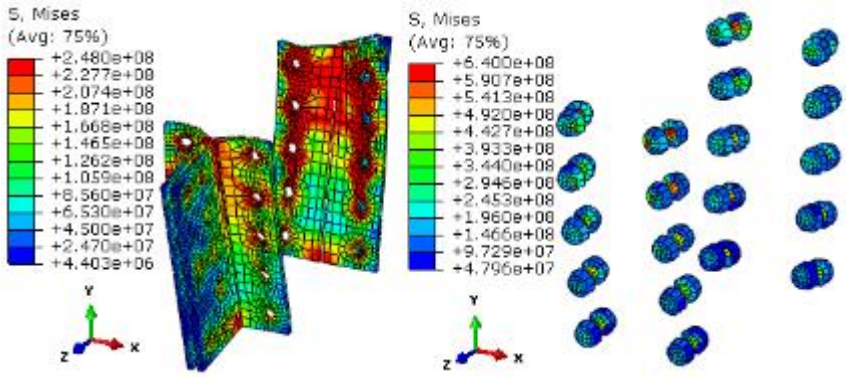

Figure 15. Connection deformation and Von-Misses Stress plot of specimen FK-5.

Numerical results for the calculated loads and displacements are shown in Table 7.

Table 7. Load versus and displacement (D_y) for specimen FK-5.

Load-Step	Displacement -D_y (m)	Load (kN)
1	0.0000000	0.000
2	0.0003211	9.000
3	0.0006580	18.000
4	0.0011517	31.507
5	0.0018886	51.754
6	0.0050622	82.123
7	0.0071695	93.514
8	0.0114548	110.606
9	0.0133329	117.014
10	0.0167126	126.619
11	0.0242357	141.034
12	0.0260660	144.000

The total vertical displacement against the total load factor graph for specimen FK-5 as shown in Figure. 16. These diagrams are used to calculate the rotation of the beam and the column.

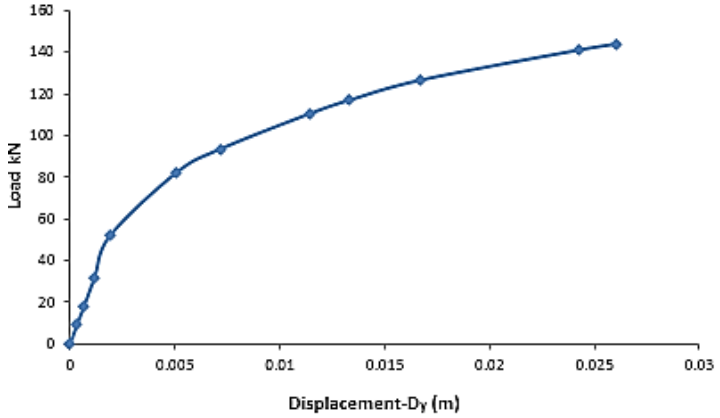

Figure 16. Load -versus vertical displacement D_y for specimen FK-5.

The result, calculated rotations Ø and moments from the computer analysis are shown in Table 8.

Table 8 Calculated moments and corresponding rotations for specimen FK-5.

Load-Step	D_{xt} (m)	D_{xb} (m)	$[\Delta_x/h]$	M (kN.m)	Ø (rad)
1	0.00000000	0.00000000	0.000000	0.000	0.000000
2	0.00011042	-0.00002933	0.000262	5.400	0.000262
5	0.00022926	-0.00005749	0.000538	10.800	0.000538
4	0.00040318	-0.00009866	0.000942	18.904	0.000941
5	0.00066314	-0.00015955	0.001544	31.052	0.001543
6	0.00177142	-0.00043705	0.004143	49.274	0.004141
7	0.00250457	-0.00062543	0.005872	56.108	0.005869
8	0.00398712	-0.00102393	0.009402	66.364	0.009397
9	0.00463671	-0.00120039	0.010951	70.209	0.010946
10	0.00580824	-0.00151561	0.013741	75.972	0.013734
11	0.00843281	-0.00221190	0.019971	84.620	0.019961
12	0.00907059	-0.00238372	0.021490	86.400	0.021479

Experimental data were obtained from Lewitt et, al., [11]. This data was modeled and analyzed by the Abaqus program. The M-Ø diagram is drawn for both the large-scale experimental test results and the Abaqus analysis results, and the yield moments of the links are determined by the intersection of the two tangents as shown in Figure 17.

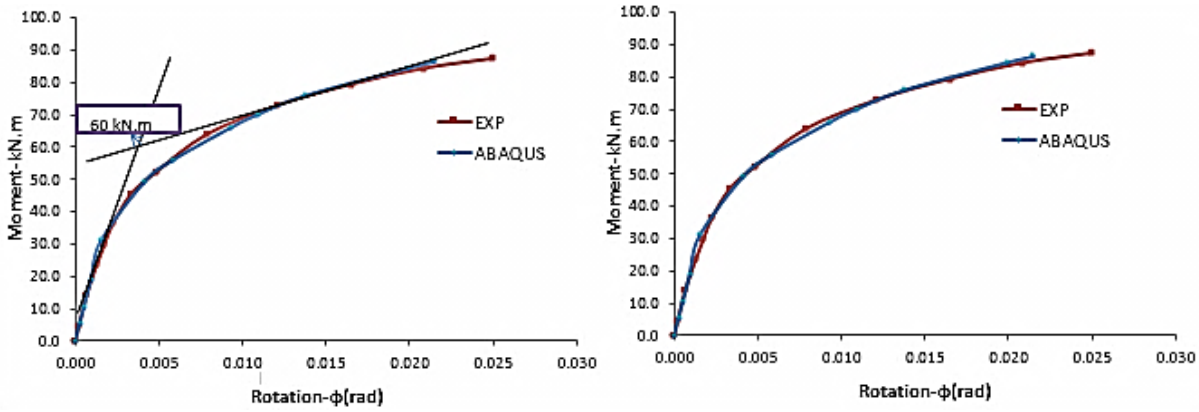

Figure 17. Moment-Rotation (M-Ø) curve for specimen FK-5.

4. Discussion of Results

Based on the charts shown in Figure 13, Figure 17 and analysis results; summary of the results for both specimens of DWA connections are shown in Table 9.

Table 9. Summary of the results for specimens FK-3 and FK-5.

Test Ref	Yield moment Kn.m		Ultimate moment Kn.m		Displacement m	
	Aba	Exp	Aba	Exp	Aba	Exp
FK-3	12.44	12.22	18.9	18.11	0.03	0.025
FK-5	60	60	86	87	0.026	0.025

Referring to Figure 13, Figure 17, and Table 8, it was found that the determination of yield moment of the connection according to computer analysis software; ABAQUS, is against the experiment, with a difference of 1.80 % for the specimen FK-3 while, in the specimen, FK-5 was 0.00 %. In addition, from the ABAQUS software analysis, the yield moment was higher than the experimental test and the ultimate moment is higher than the experimental test for the specimen FK-3. Whereas, in the specimen FK-5, the yield moment was almost equal than the experimental test and the ultimate moment is higher than the experimental. Furthermore, the ultimate moment values from computer analysis were very close from the experiment for both specimens. moreover, the displacement of computer analysis is more than the experience by a very simple difference. Finally, it can also be noted that the computer model seems to be stiffer than the experimental model at lower loads up to the yield moments, after which the experimental model showed stiffer than the ABAQUS numerical results in the specimen FK-5. The results of this study identify weaknesses in connections that can be overcome sand strengthened to improve the behaviour of such connections. For example, the diameter of the bolts of the specimen FK-3 and FK-5 connection, which fails in the fault mode at the all angles connection, can be increased from 19 mm to 20 mm. This solution increases the strength of communication, especially since the rest of the elements of communication did not collapse and has the ability to withstand longer. Moreover, the angular thickness of the specimen FK-3 connections, which fails in the fault mode at the top of web angle, can be increased from 9.5 to 11 mm. In addition, for the specimen FK-5 with an angular thickness of 11.1 mm and a failure mode at the top of web angle and bolts, the thickness can be increased from 11.1 mm to 12 mm.

5. Conclusion

This paper reports on the DWA connections, a finite element model using ABAQUS in order to investigate the performance of DWA connections steel at room temperature. Validation of the numerical modelling against all representative experimental results conducted on the moment-rotation relationship, final deformation and yield line pattern of the DWA connections shows good agreements exist. For this reason, this numerical analysis method can be used safely to predict the behavior of DWA steel beam-column connections at room temperature. The following conclusions can be drawn. The difficulty of numerical modeling contact interactions taking into account the material and non-linear geometric

effects has been successfully solved. The proposed DWA model is verified to simulate DWA steel connections up to the maximum moment at room temperature. Accordingly, modeling DWA can be used to predict stress distribution of high strength steel DWA connections both at ambient temperature, which is not easy to achieve in full-scale tests, via inputting proper mechanical properties of high strength steels at ambient temperature. By the current modeling approach, the first critical component of DWA links can be identified, only the occurrence of component breakdown and subsequent failures of other components cannot be predicted. Finally, the load bearing capacity, as well as rotation capacity of DWA connections, is dependent on the thickness of angle and numbers of bolts. By the way, all connection studies, that use finite element analysis using computer software provides a lot of effort and money, as compared to a large-scale test, and can produce a complete picture of the behavior of joints and deformation, tension and distribution of power and stress.

Acknowledgments
The authors would like to thank the two anonymous reviewers for their constructive comments that have enhanced the quality of the paper. This work was supported by the Ministry of Higher Education and the University of Malaysia Pahang (UMP) and the authors would like to thank them for their support.

References

[1] Prabha P, Rekha S, Marimuthu V, Saravanan, M, Palani G S and Surendran M 2015 Modified Frye–Morris polynomial model for double web-angle connections *International Journal of Advanced Structural Engineering (IJASE)* **7**(3) 295-306
[2] Ghindea M, Catarig A and Ballok R I 2015 Semi-Rigid Behaviour Of Bolted Connections Using Angle Cleats Part 1. Development Of 3-D Finite Element Model *Buletinul Institutului Politehnic din lasi. Sectia Constructii, Arhitectura* **61**(4) 53
[3] Ahmed A and Hasan R 2015 Effect and evaluation of prying action for top-and seat-angle connections *International Journal of Advanced Structural Engineering* (IJASE) **7**(2) 159-169
[4] Sulong N R, Elghazouli A Y, Izzuddin B A and Ajit N 2010 Modelling of beam-to-column connections at elevated temperature using the component method *Steel and Composite Structures*, **10**(1) 23-43
[5] Abolmaali A, Kukreti A R and Razavi H 2003 Hysteresis behavior of semi-rigid double web angle steel connections *Journal of Constructional Steel Research* **59**(8) 1057-1082
[6] Xinwu W 2007 Experimental research on hysteretic behavior of top-seat and web angles connections. In 5th WSEAS International Conference on Environment, Ecosystems and Development, Tenerife, Spain (pp. 14-16)
[7] Liew J R, White D W and Chen W F 1993 Limit states design of semi-rigid frames using advanced analysis: Part 1: Connection modeling and classification *Journal of Constructional Steel Research* **26**(1) 1-27
[8] Liew J R, White D W and Chen W F 1993 Limit states design of semi-rigid frames using advanced analysis: Part 1: Connection modeling and classification *Journal of Constructional Steel Research* **26**(1) 1-27
[9] Hong K, Yang J G and Lee S K 2002 Moment–rotation behavior of double angle connections subjected to shear load *Engineering Structures* **24**(1) 125-132
[10] Chen W F 2011 Semi-rigid connections handbook. J. Ross Publishing, pp 23-32.
[11] Lewitt C W, Chesson Jr E, & Munse W H 1966 Restraint characteristics of flexible riveted and bolted beam-to-column connections. University of Illinois Engineering Experiment Station. College of Engineering. University of Illinois at Urbana-Champaign.
[12] Pirmoz A, Khoei A S, Mohammadrezapour E and Daryan A S 2009 Moment–rotation behavior of bolted top–seat angle connections *Journal of Constructional Steel Research* **65**(4) 973-984
[13] Danesh F, Pirmoz A and Daryan A S 2007 Effect of shear force on the initial stiffness of top and seat angle connections with double web angles *Journal of Constructional Steel Research* **63**(9), 1208-1218
[14] Hean L S, Sulong N R and Jameel M 2016 Effect of axial restraints on top-seat angle connections at elevated temperatures *KSCE Journal of Civil En*gineering **20**(6) 2375-2383

[15] Daryan A S and Yahyai M 2009 Behavior of bolted top-seat angle connections in fire *Journal of Constructional Steel Research* **65**(3) 531-541
[16] Stelmack T W, Marley M J and Gerstle, K. H 1986 Analysis and tests of flexibly connected steel frames *Journal of Structural Engineering* **112**(7) 1573-1588
[17] Kukreti A R and Abolmaali A S 1999 Moment-rotation hysteresis behavior of top and seat angle steel frame connections *Journal of Structural Engineering* **125**(8) 810-820
[18] Dai X H, Wang Y C and Bailey C G 2010 Numerical modelling of structural fire behaviour of restrained steel beam–column assemblies using typical joint types *Engineering Structures* **32**(8) 2337-2351
[19] Azizinamini A and Radziminski J B 1989 Static and cyclic performance of semirigid steel beam-to-column connections. *Journal of Structural Engineering* **115**(12) 2979-2999.